BRANZ
THE RESOURCE CENTRE FOR BUILDING EXCELLENCE

REPRINT

No 138(1996)

Design of Light Steel-Framed Walls for Fire Resistance

J.T. Gerlich, P.C.R. Collier
and A.H. Buchanan

From: Fire and Materials, Vol. 20,
79-96 (1996)

Funding for the work presented here was provided by the Foundation for Research, Science and Technology from the Public Good Science Fund; the Building Research Levy; and Winstone Wallboards Ltd, Auckland.

ISSN: 0111-7459

FIRE AND MATERIALS, VOL. 20, 79–96 (1996)

Design of Light Steel-framed Walls for Fire Resistance

J. T. Gerlich
Systems Technology Manager, Winstone Wallboards Ltd, P.O.Box 36024, Moera, Lower Hutt, New Zealand

P. C. R. Collier
Fire Research Engineer, Building Research Association of New Zealand, Private Bag 50908, Porirua, New Zealand

A. H. Buchanan
Associate Professor, Department of Civil Engineering, University of Canterbury, Private Bag 4800, Christchurch, New Zealand

Light steel-frame building systems are becoming more prevalent in commercial, industrial and residential construction in New Zealand. Tested fire resistance ratings are generally available for non-load-bearing systems, but not for load-bearing applications. This study investigates the performance of load-bearing light steel-frame systems exposed to fire. Methods are presented for calculating the reduction of steel strength and stiffness at elevated temperatures, and for predicting the deflections resulting from temperature gradients and P-Δ effects. Heat transfer modelling by computer is used to predict steel framing temperatures for systems exposed to the standard ISO 834 time–temperature curve and real fires. Three full-scale furnace tests were carried out to evaluate analytical predictions. A design procedure is proposed.

INTRODUCTION

The traditional method of interior wall construction in New Zealand is with light timber framing and sheet material linings. Paper-faced gypsum plasterboard linings are most commonly used, particularly when a fire resistance rating is required. Construction in cold-formed light steel framing (LSF) is not as well established as in the USA and Australia, but there is increasing competitiveness of LSF against timber framing. Recent building code reforms have created market opportunities for framed systems (both timber and steel) in low-rise industrial and commercial construction, previously the preserve of concrete construction.

The growth of LSF systems is expected to increase the demand for economical solutions where specific performance is required, such as in the area of fire resistance. Non-load-bearing LSF systems have an established history of use, mainly in light industrial and commercial partitioning. Load-bearing LSF systems are most likely to be part of a total LSF construction system. With the developing use of LSF in load-bearing applications, the demand for systems with fire resistance ratings has increased.

Fire testing against standard time–temperature furnace conditions will give good comparative data for systems tested under identical conditions. However, standard fire resistance tests do not accurately model the performance of a building element when exposed to a real fire. An analytical model is needed to permit calculation of the expected fire performance of LSF systems exposed to both standard fires and real fires.

In real fires the fire growth phase, steady state and decay depend on aspects such as the total fuel load in the fire compartment, fuel type and configuration, compartment size and ventilation openings, and thermal properties of building materials. A comparison between the standard ISO 834[1] curve and two possible real fires is given in Fig. 1. The real fires represent a hydrocarbon pool fire with a rapid growth, short duration and rapid decay phase, and a fuel bed controlled wood crib fire with a slow temperature rise, long duration and slow decay.

The aim of this study was to develop an understanding of the performance of load-bearing LSF walls and to model the performance against standard ISO 834[1] and real compartment fires by;

- Carrying out a survey of existing literature
- Comparing and verifying existing structural design approaches at room temperature
- Predicting steel temperatures within cavity walls
- Determining the effects of elevated temperature on structural performance
- Verifying the model with full-scale loadbearing fire resistance tests.

More details of the study are given by Gerlich.[2]

STRUCTURAL MODEL

In order to predict the structural behaviour of load-bearing LSF systems exposed to elevated temperatures experienced in fires it is first necessary to develop an understanding of the performance at room temperature. Of particular interest is the ultimate limit state condition as the fire design is expected to be governed by structural collapse.

Construction details

One of the main advantages of cold-formed light steel framing is the ability to form galvanized steel coil into

CCC 0308–0501/96/020079–18

Received 4 July 1995
Accepted 5 December 1995

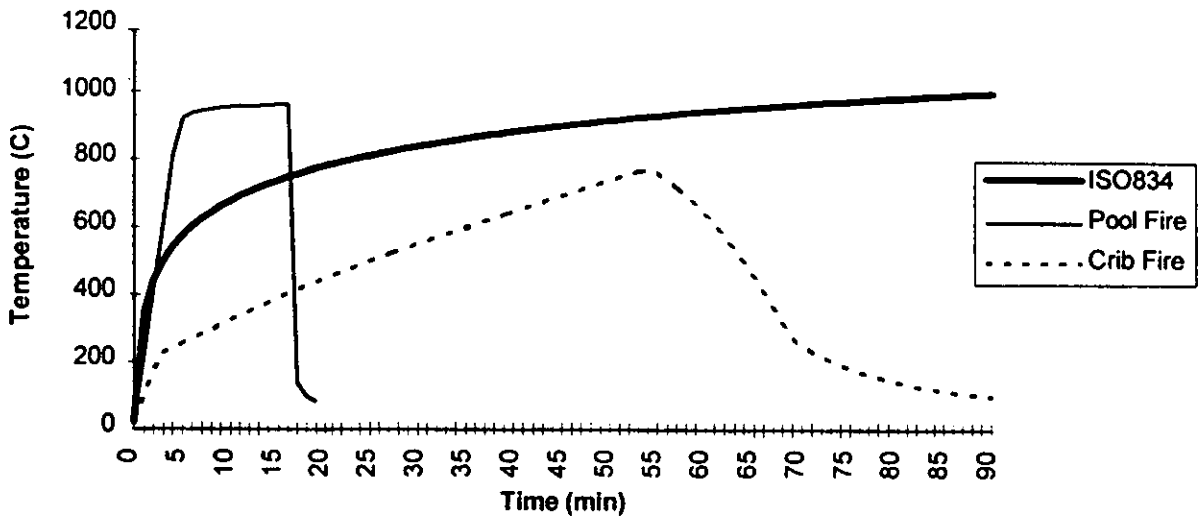

Figure 1. Comparison of possible real fires with the standard ISO 834 curve.

any shape of stud and channel sections, tailored to meet particular requirements. For load-bearing applications simple C-section bottom channels and studs are most commonly used. Top channels can be C-sections or special sections formed to provide additional span capability, as shown in Fig. 2. The steel base metal thickness is commonly in the range from 0.7 to 1.6 mm depending on the application.

In load-bearing applications a positive stud to channel fixing is required to transfer the applied axial loads. The steel framing industry has typically used screws or welded connections. More recently tab-in-slot and clinching methods have also been used. Common details are shown in Fig. 3.

Restraint conditions

Under room temperature conditions, lateral restraint against torsional buckling and buckling about the minor axis is provided by sheet lining materials such as gypsum-based plasterboard. However, the properties of lining materials change significantly when exposed to fire temperatures. Degradation of the lining on the fire-exposed side will reduce its ability to prevent buckling of the studs when steel temperatures reach critical levels (> 300–400°C). In the design of fire-rated steel-framed systems the lateral restraint provided by the linings on the fire side must be ignored when assessing fire-induced ultimate limit state conditions.

Structural design codes

The behaviour of thin cold-formed sections is significantly different from that of hot-rolled structural steel and special design considerations are required. Typical problems encountered in the structural design of cold-formed steel compression members are illustrated in Fig. 4 and include local buckling of thin plate elements and the susceptibility to torsional flexural buckling due to a low torsional stiffness.

To predict the limit state condition of cold-formed steel structures at room temperature, three design codes were compared: AS 1538,[3] BS 5950,[4] and the AISI[5] design manual. The AISI manual was found to give the most accurate failure predictions. Although cumbersome, the AISI design manual equations lend themselves to solution by spreadsheet.

Structural testing

In order to calibrate the analytical design method, structural testing for material yield strength and combined axial loading and bending was carried out at room temperature. This testing also served to determine more accurately the cold capacity and failure mode of specimens prior to full-scale fire testing.

To establish the yield strength of the steel framing material, tensile and compressive stub-column tests were carried out in accordance with AS 1538. The tensile test specimens were fitted with strain gauges and continuous load-deflection plots were obtained. The short stub-column specimens were loaded in compression. The results established that yield strengths of 300 MPa and 450 MPa were applicable for the $75 \times 32 \times 1.15$ mm and $100 \times 50 \times 1.0$ mm stud C-sections respectively. These values were then used in designs according to the AISI manual.

Full length (3 metre) specimens were tested under combined axial loading and bending to confirm the reliability of the AISI design method. Both lined and unlined specimens were tested.

The test set-up is shown in Fig. 5. Specimens were mounted horizontally and the axial load was applied by a manually operated hydraulic jack at the top channel level through a heavy structural steel spreader beam supported on rollers. At the bottom channel level the reaction was provided by a rigid continuous support which was securely bolted to the reaction floor.

Predicted failure loads calculated in accordance with the AISI limit state design method showed reasonable agreement when compared with test results. The AISI design manual generally gives conservative predictions of maximum axial loads.

The perceived complexity of LSF design codes results from the potential for local buckling failures of thin members. The likelihood of buckling was confirmed by the observed failure of the top-hat section in the first test series. Careful load-path analysis is required. This

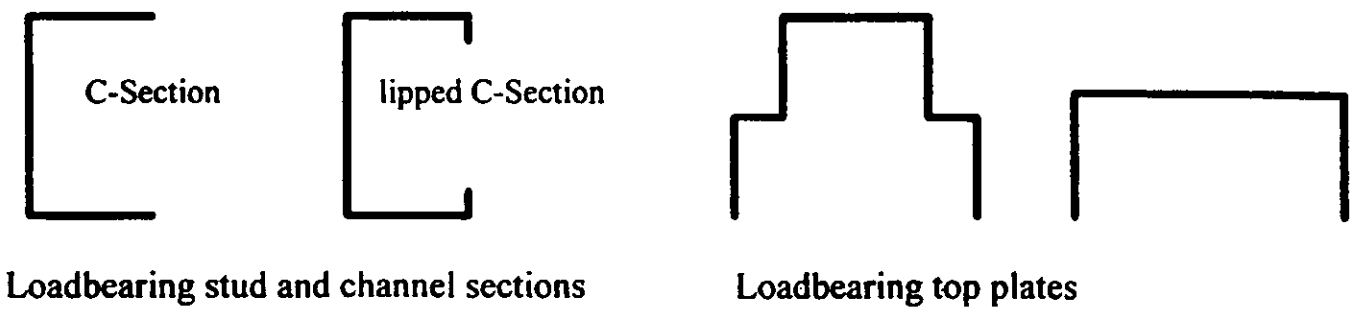

Figure 2. Common steel framing sections.

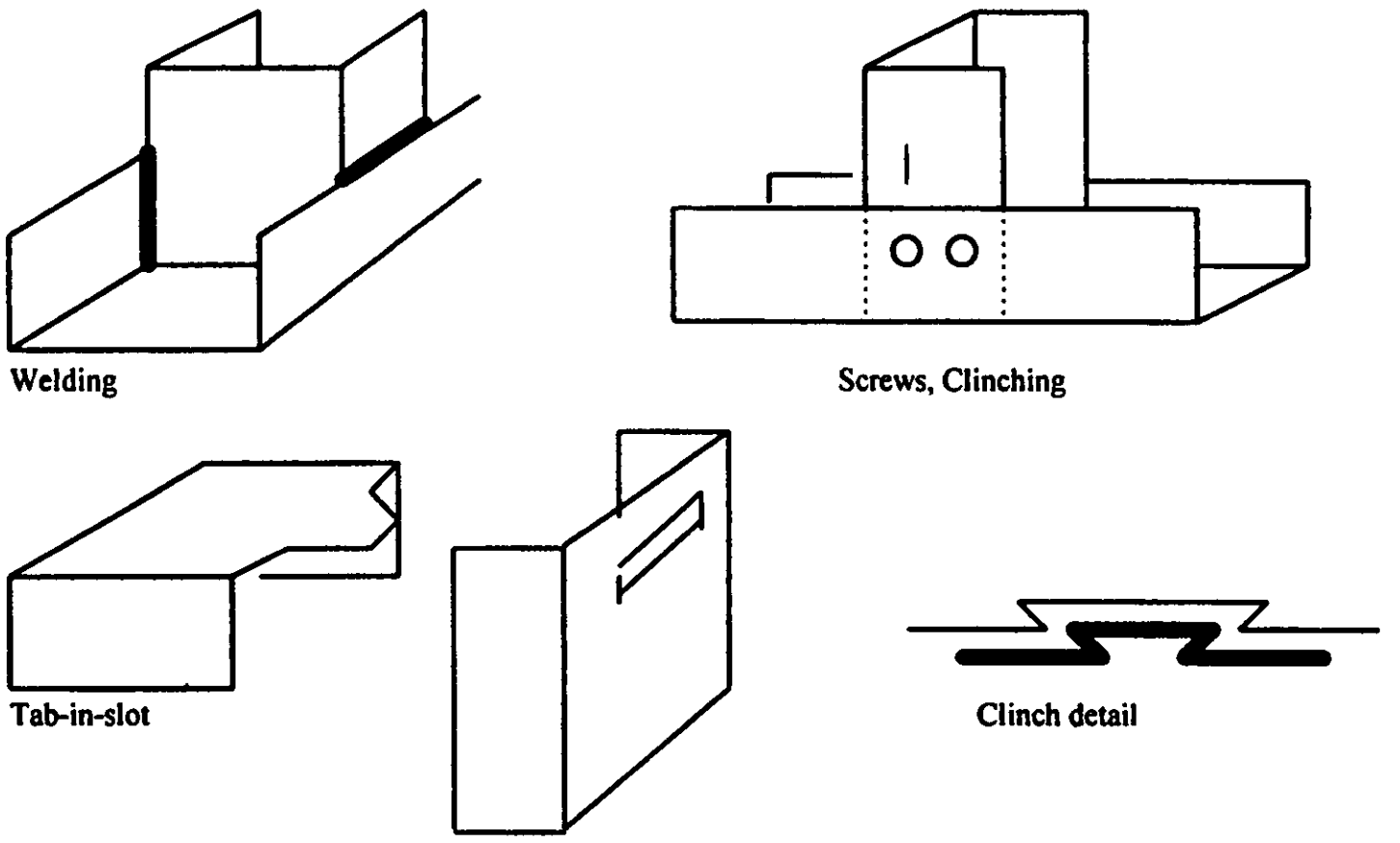

Figure 3. Typical stud to channel connections.

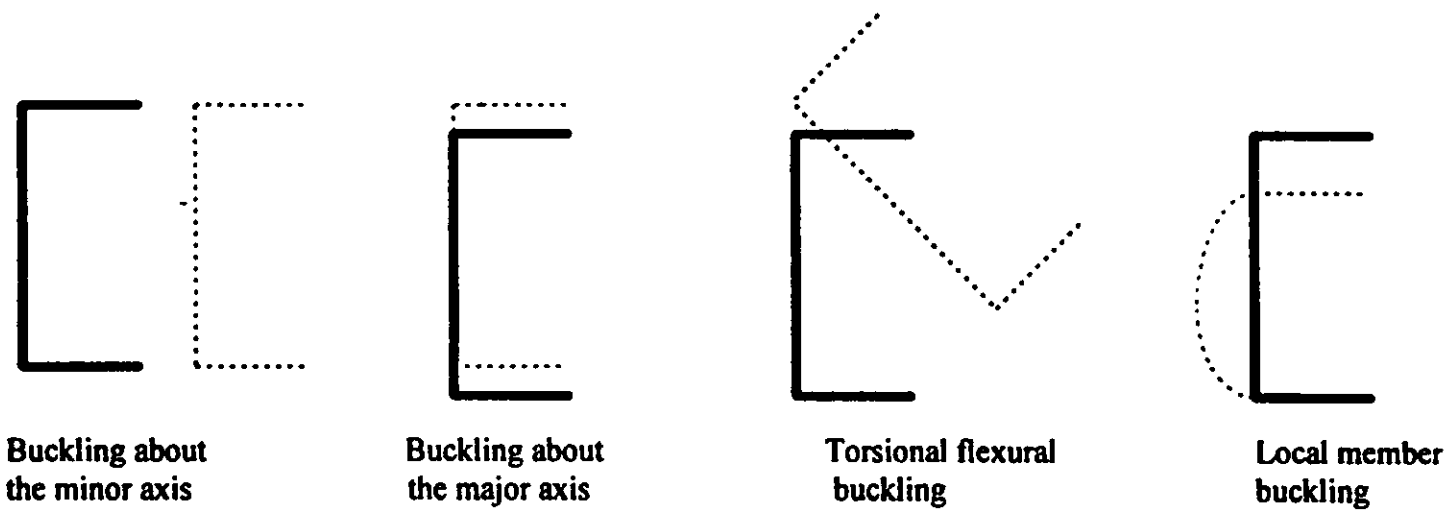

Figure 4. Buckling modes of cold-formed steel members.

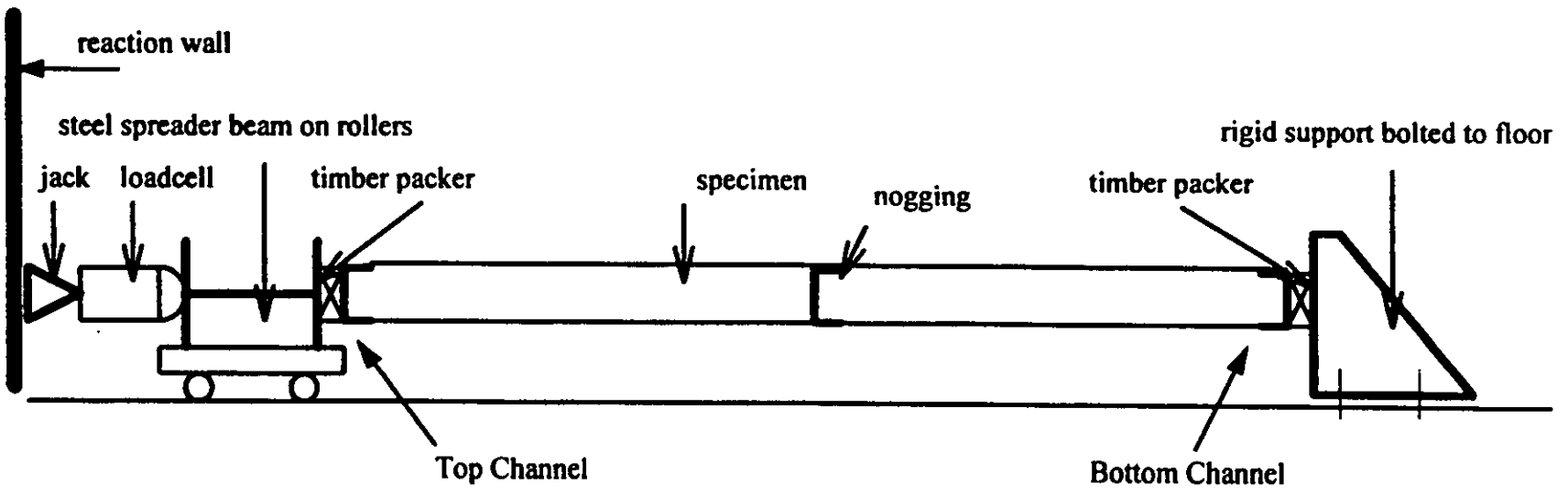

Figure 5. Test set-up for combined axial loading and bending.

characteristic is recognized by most literature on the design of cold-formed steel structures, as well as by the cold-formed steel design codes.

TEMPERATURE EFFECTS

The dominant consideration when assessing the fire performance of load-bearing LSF systems is the effect of elevated temperature on the behaviour and material properties of the steel stud wall components. The failure scenario is determined by the performance of gypsum plasterboard linings, the cold-formed steel properties at elevated temperatures and considerations such as increased P-Δ effects due to thermally induced deflections.

Properties of gypsum plasterboard linings at elevated temperatures

Gypsum plasterboard linings are commonly used to provide fire resistance in framed construction. When exposed to fire the free water and chemically combined water in the gypsum is gradually driven off at temperatures above 100°C. This causes a temperature plateau on the unexposed face of the lining. The length of this plateau is a function of the lining thickness, density and composition. As temperatures rise above 100°C, calcination of the gypsum plaster severely reduces its strength. At room temperature screw-fixed gypsum plasterboard linings provide adequate restraint against lateral buckling of the steel studs about the minor axis. During exposure to fire this ability to provide lateral restraint diminishes as the thickness of undamaged gypsum progressively decreases.

When steel temperatures on the hot side of the wall assembly reach critical levels the exposed plasterboard lining will no longer provide lateral restraint. In comparison, the lining on the cold side of the assembly will degrade to a lesser degree, and its ability to provide lateral restraint will depend on the remaining thickness of undamaged material.

Thomas *et al.*[6] summarize data measured by Mehaffey[7] for the thermal conductivity and enthalpy of glass–fibre reinforced gypsum plasterboard as a function of temperature. Thomas's values for the thermal conductivity of gypsum plasterboard are presented in Fig. 6. Enthalpy values are given in Fig. 7 and represent the summation of the product of specific heat and temperature, expressed per unit of volume. Enthalpy values are used in modelling to avoid numerical instabilities resulting from the sharp peaks that may occur in the specific heat of materials containing water, due to evaporation of moisture.

Properties of cold-formed steel at elevated temperatures

The mechanical and thermal properties of steel are of interest when considering the behaviour at elevated

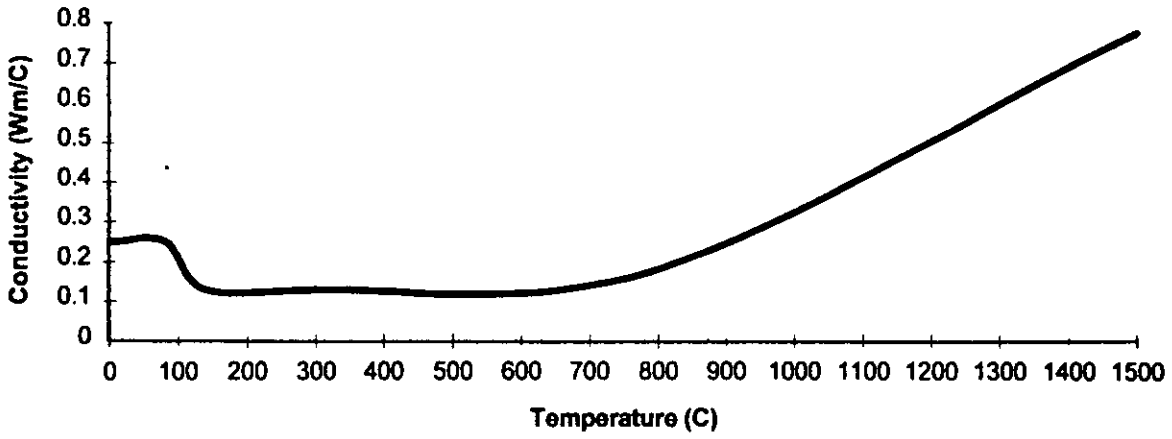

Figure 6. Thermal conductivity of gypsum plasterboard.

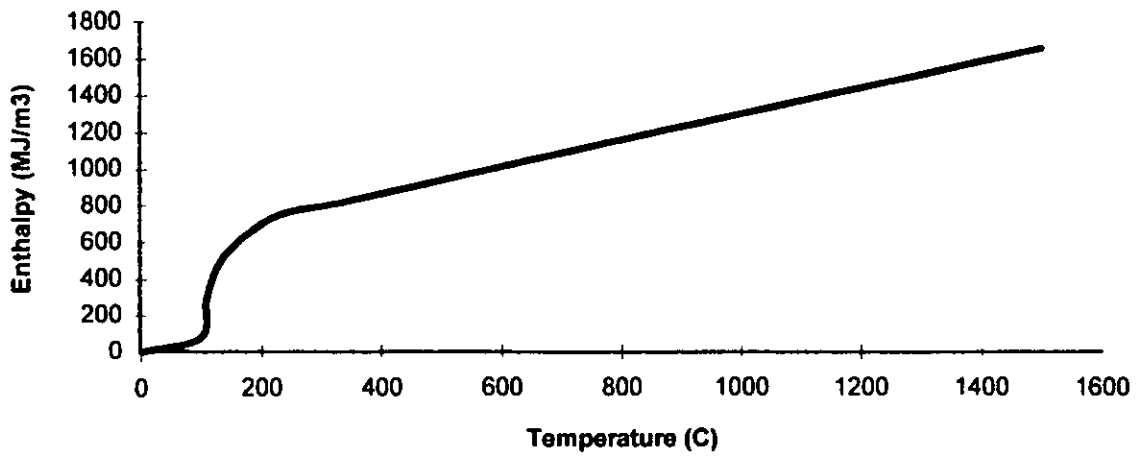

Figure 7. Specific volumetric enthalpy of gypsum plasterboard.

temperatures. Significant mechanical properties are the density, yield strength, modulus of elasticity and coefficient of thermal expansion. Relevant thermal properties are the specific heat and thermal conductivity. With the exception of density, all these parameters are strongly influenced by temperature. In addition, the crystalline structure of carbon steels typically used in construction also changes at temperatures above approximately 650°C. However, failure of load-bearing LSF systems is expected before crystalline steel structure changes become a factor.

Mechanical properties. Klippstein,[9] on behalf of the AISI, carried out experimental work on the yield strength as a function of temperature for cold-formed steel framing members. The data found by Klippstein was used to fit a polynomial which gives

$$F_{yT}/F_{y0} = 1 - 5.3T/10^4 + 4.0T^2/10^6 - 1.9T^3/10^8 + 1.7T^4/10^{11} \quad (1)$$

where

F_{yT} is the yield stress (MPa) at temperature T (°C)
F_{y0} is the yield stress (MPa) at room temperature (≈ 20°C)
T is the temperature of the steel (°C)

Klippstein[9] presents experimentally derived data for the modulus of elasticity for cold-formed steel studs. For this study a polynomial was fitted to this data which gives

$$E_T/E_0 = 1 - 3.0T/10^4 + 3.7T^2/10^7 - 6.1T^3/10^9 + 5.4T^4/10^{12} \quad (2)$$

where

E_T is the modulus of elasticity (MPa) at temperature T (°C)
E_0 is the modulus of elasticity (MPa) at room temperature (20°C)

The effect of temperature on the coefficient of thermal expansion of steel is stated by Lie[10] as

$$\alpha_T = (0.004T + 12) \times 10^{-6}, \quad \text{for } T < 1000°C \quad (3)$$

where

α_T is the coefficient of thermal expansion at temperature T (°C $^{-1}$)

Thermal properties. The temperature rise of a steel member as a result of heat flow is a function of the thermal conductivity and specific heat of the material. The approximation for the thermal conductivity as a function of temperature is given by the following equation:[10]

$$k = -0.022T + 48, \quad \text{for } 0 < T < 900°C \quad (4)$$

where k is the thermal conductivity (W/m°C).

The specific heat (c) for most steels increases gradually with temperature. A constant value of 600 J/kg°C is suggested for temperatures below 600°C.[10,11] For this study, data for higher temperatures are not required as stud failure is expected to occur at temperatures below 600°C.

Thermal deflections. Cooke[12] considers the thermal bowing of simply supported steel members due to a temperature gradient across the section and derives the following expression for mid-span deflection,

$$\Delta_1 = \frac{\alpha L^2 \delta T}{8D} \quad (5)$$

where,

Δ_1 is the mid-span deflection due to thermal bowing (mm)
α is the thermal expansion coefficient for steel (°C^{-1})
L is the member length (wall height) (mm)
δT is the temperature difference across the member (°C)
D is the member depth (mm)

Tests described later in this paper show that at relatively moderate temperatures (< 400°C) Eqn (5) reasonably predicts the mid-span deflection, provided that the steel studs are free to rotate and expand at both ends. At higher temperatures the correlation between measured and calculated deflections is less accurate. After longer fire exposure the temperature difference across the steel member reduces but actual deflections do not return to the calculated levels because of plastic deformations of the steel.

P–Δ Effects. With load-bearing systems additional horizontal deflections will occur as a result of P-Δ effects. The stress-free thermal deflection can be treated as an initial eccentricity (Δ_1). The initial bending moment $P\Delta_1$ results in a further horizontal deflection Δ_2, illustrated in Fig. 8.

The total horizontal displacement ($\Delta_1 + \Delta_2$) of the member will be the sum of the thermal deflection and the deflection due to P-Δ effects. The P-Δ component may be predicted analytically by solving the following moment equilibrium equation:

$$E_T I_x \frac{d^2\Delta_2}{dz^2} = P_a(\Delta_1 + \Delta_2) \quad (6)$$

The solution to this equation for Δ_2 at mid-height is obtained as[2]

$$\Delta_2 = \Delta_1 \left[\frac{1}{\cos\frac{\mu L}{2}} - 1 \right] \quad (7)$$

where,

E_T is the elastic modulus of steel as a function of temperature (MPa)
I_x is the second moment of area of the cross-section (mm^3)
P_a is the applied axial load (N)
Δ_1 is the initial eccentricity (thermal deflection) (mm)
Δ_2 is the P-Δ deflection (mm)
z is the stud height (mm)
μ is $\sqrt{\frac{P_a}{E_T I_x}}$ (mm^{-1})
L is the wall height (mm)

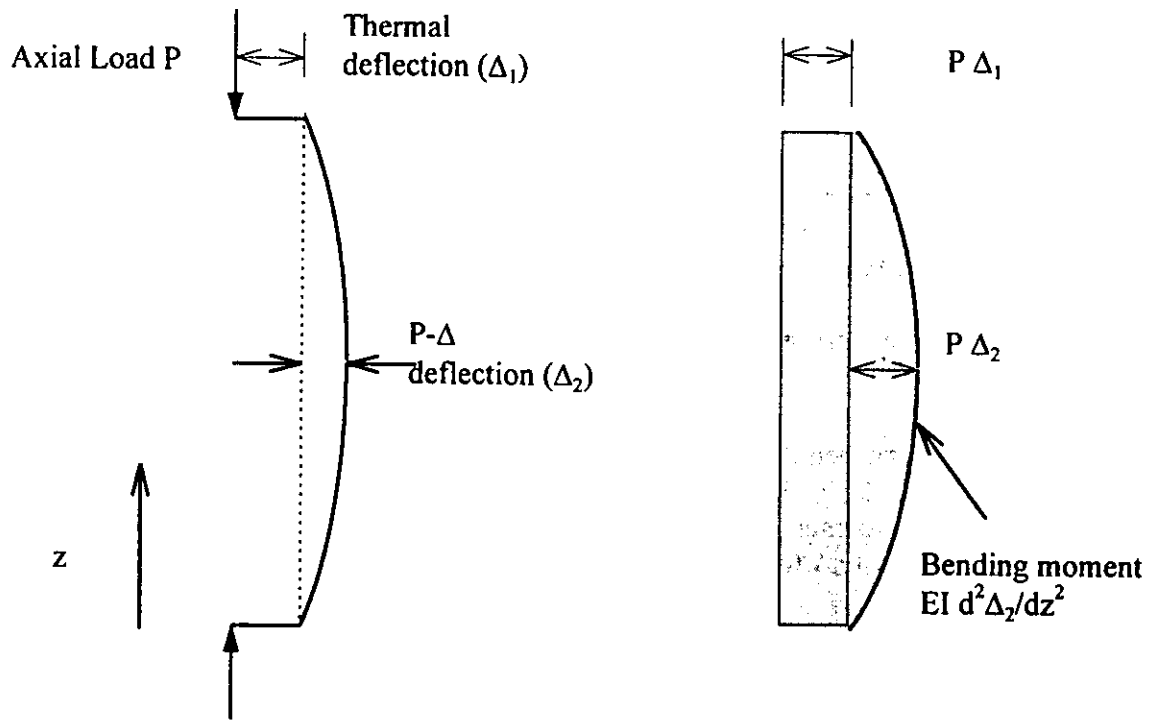

Figure 8. Total horizontal deflection for load-bearing systems.

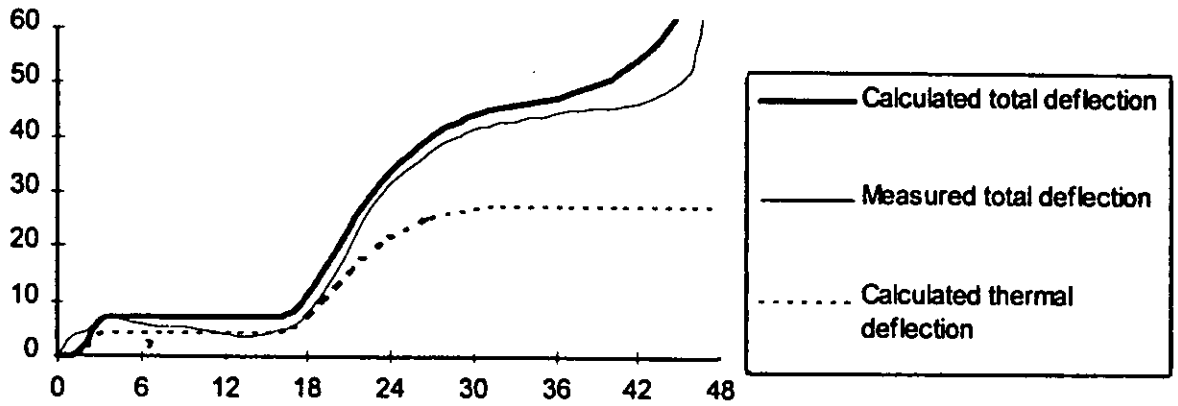

Figure 9. Comparison between calculated and measured horizontal deflections (test 2).

The measured curvature of the steel studs at various time intervals during full-scale furnace tests is discussed later in this paper. For the details used in this study it is concluded that moments at the stud end-fixings are insufficient to significantly reduce thermal deflections below those predicted for pinned end conditions. The thermal deflections are hence calculated using Eqn (5) assuming pinned joints. These deflections are entered as the initial eccentricity to calculate the P-Δ deflection in accordance with Eqn. (7).

Good agreement was achieved between the deflections calculated from measured temperatures, and the measured horizontal deflections. Figure 9 shows the comparison for test 2. The tests are described later in this paper.

THERMAL MODEL

Proprietary heat transfer models for timber-framed cavity systems are currently being developed in New Zealand by Collier[13] and in Australia by Clancy *et al.*[14] These models show promising correlation when compared with actual fire test results. It is anticipated that these proprietary models can be modified for steel-framed systems by adjusting the thermal properties of the framing from timber to steel.

Thomas *et al.*[6] describe the use of the commercially available heat transfer model TASEF[15] to predict the performance of light timber-framed walls exposed to standard ISO 834[1] fires and real compartment fires. TASEF was used to predict the heat transfer and steel framing temperatures in this study.

TASEF input

TASEF is a two-dimensional finite element program designed to model heat transfer through materials and composite construction elements exposed to any fire. A fine mesh will produce more accurate results, but at the expense of more computing time. Figure 10 shows the finite element mesh which was found to give reasonably accurate results at realistic program run times (approximately 40 minutes on an IBM-compatible 486PC).

TASEF requires material input data for each region except for voids. Conductivity and specific volumetric

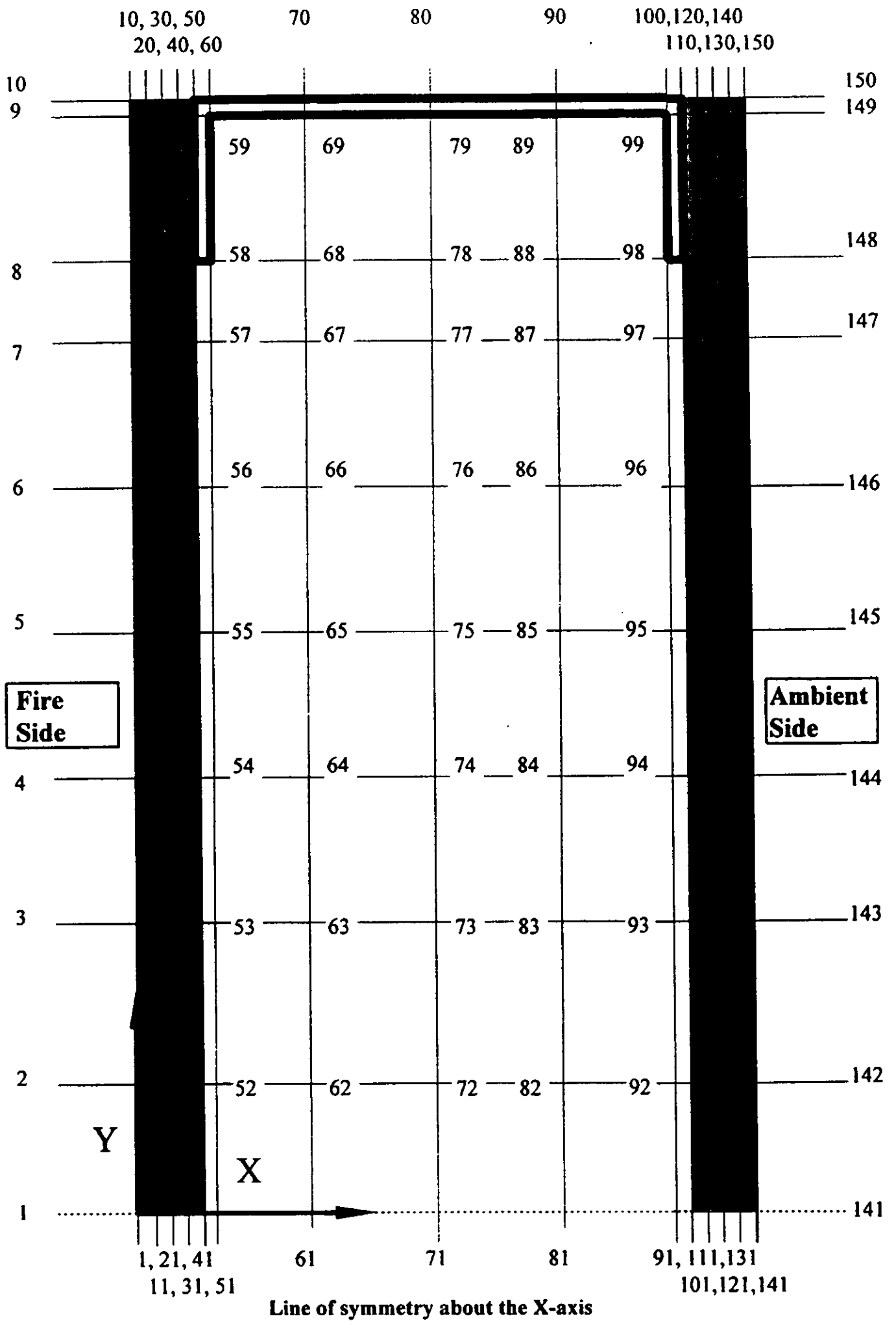

Figure 10. Typical finite element mesh for the thermal model using TASEF.

enthalpy need to be supplied as a function of temperature. The program has a database for standard thermal properties of common construction materials such as steel and concrete. These properties were assigned to the steel framing members. Proprietary data were entered for the gypsum lining material.

The heat transfer at boundaries between solid materials and gases is governed by the equation

$$q = \varepsilon\sigma(T_g^4 - T_s^4) + \beta(T_g - T_s)^\gamma \qquad (8)$$

where

q is the rate of heat transfer ($W\,m^{-2}$)
ε is the resultant emissivity of the gas and the boundary (dimensionless)
σ is the Stefan–Boltzmann constant ($5.67*10^{-8}$ $W\,m^{-2}K^4$)
β is the convection coefficient ($W\,m^{-2}K^\gamma$)
γ is the convection power (dimensionless)
T_g is the gas temperature (K)
T_s is the surface temperature (K)

The values used for the boundaries (from Thomas *et al.*[6]) are presented in Table 1.

TASEF output

The output from TASEF was compared with test results. The temperature measurement positions are illustrated

in Fig. 11. The comparison between predicted and measured steel temperatures is illustrated in Fig. 12. Heavy lines indicate the results from the furnace tests and the lighter lines indicate the predictions using the TASEF model.

TASEF does not model mass transfer (moisture movement). As a result, a discrepancy occurs at the ambient side of the wall assembly at temperatures below 120°C. The lining on the fire side of the cavity is losing water due to evaporation. The ambient side of the cavity is heated by moisture condensing on it. The energy input from condensation is equal to the energy required to evaporate it again later. The overall effect has been found to be negligible.[6]

At very high temperatures, some opening of the exposed sheet joints due to deflection of the framing members and ablation (erosion due to heating) of the exposed linings will allow hot gases into the cavity. These effects result in an accelerated rise in measured temperatures towards the end of the tests and are not modelled by TASEF. As a result, inaccuracies between predictions and measurements occur at high temperatures. For fires which are significantly hotter than the ISO 834[1] curve it is believed that a rapid rate of temperature rise and an early exposure to high temperatures results in earlier, more severe degradation of the lining. This is confirmed by Collier[13] following work on timber-framed cavity walls exposed to real fires. For this reason the TASEF temperature predictions are too low for fires which are significantly hotter than the ISO 834 conditions.

Despite the above limitations, the TASEF predictions of the temperature distribution within steel frame walls exposed to fire are reasonably accurate and within limits expected from a commercially available multi-purpose computer program. Further accuracy could be achieved by modelling for ablation.[13,14]

Table 1. Heat transfer coefficients for the TASEF model

Boundary Position	ε	β	γ
Fire side of the assembly	0.8	1.00	1.33
Lining, fire side of the cavity	0.6	1.00	1.33
Steel stud, in the cavity	0.8	1.00	1.33
Lining, ambient side of the cavity	0.6	1.00	1.33
Ambient side of the assembly	0.6	2.20	1.33

FULL-SCALE FIRE TESTING

To evaluate the performance of load-bearing LSF walls exposed to fire, three full-scale furnace tests were carried out at the laboratory of BRANZ (Building Research Association of New Zealand). Tests were in accordance with AS1530: Part 4,[16] except that the furnace temperatures for the third test were modified to give more severe exposure after about 8 minutes. For the other two tests the furnace temperature closely followed the prescribed ISO 834[1] curve.

The test specimens were constructed in a concrete-lined specimen holder 3 m wide by 4 m high. A 1 m high concrete infill panel was used above the wall in test 1. Infill plinths were bolted to the specimen holder at the top and bottom of the walls. The bottom platen of the specimen holder was free to move up and down. During the fire tests, load was applied to the wall by means of hydraulic jacks placed between the platen and the frame as illustrated in Fig. 13.

Table 2 gives an overview of the tests carried out as part of this study. All specimens consisted of welded load-bearing steel framed walls. Studs were placed at 600 mm centres and frames had a central row of nogs. A timber loading block located on the top channel section ensured loading of the central four studs only. Flanges of the top channel were cut in the end bays to minimize load transfer to the cooler edge studs and to the specimen holder.

The steel frames were lined on both faces with a single layer of glass-fibre reinforced gypsum plasterboard. The sheets were fixed vertically to all studs with self-drilling screws spaced at 300 mm centres. The vertical sheet joints were formed over studs and finished in accordance with recommended trade practice using paper tape and two coats of jointing compound. The sheet length covered the full frame height so that no horizontal joints were needed.

The specimens were loaded 30 minutes prior to the start of the fire test and load was kept constant for the duration of the test. Vertical thermal expansion of the steel framing members was allowed to occur freely. In contrast, testing described by Klippstein[9,17] in accordance with the requirements of ASTM[18] did not allow for this vertical expansion to occur and as a result the applied loads during the fire tests increased to almost twice the initial load.

Figure 14 shows the furnace temperature compared with the ISO 834[1] curve, and measured lining and steel temperatures for the three tests. Steel temperatures were recorded at 1/4 points on the four central studs. Thermocouples were attached to the steel web and to the inside of each flange, as shown in Fig. 11.

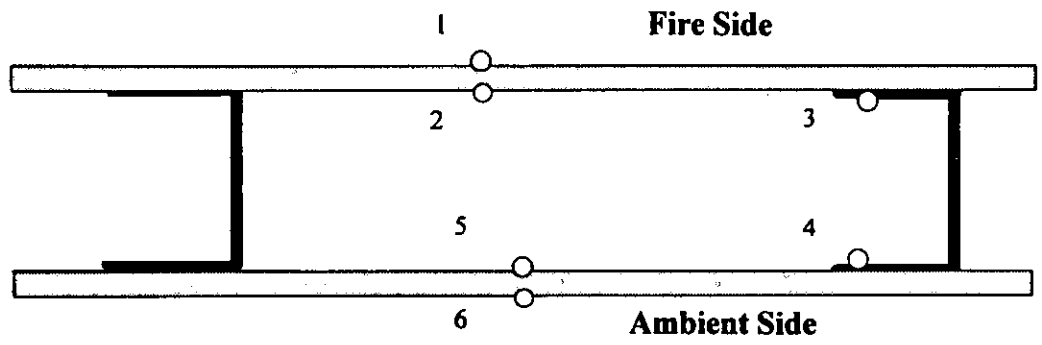

Figure 11. Temperature positions.

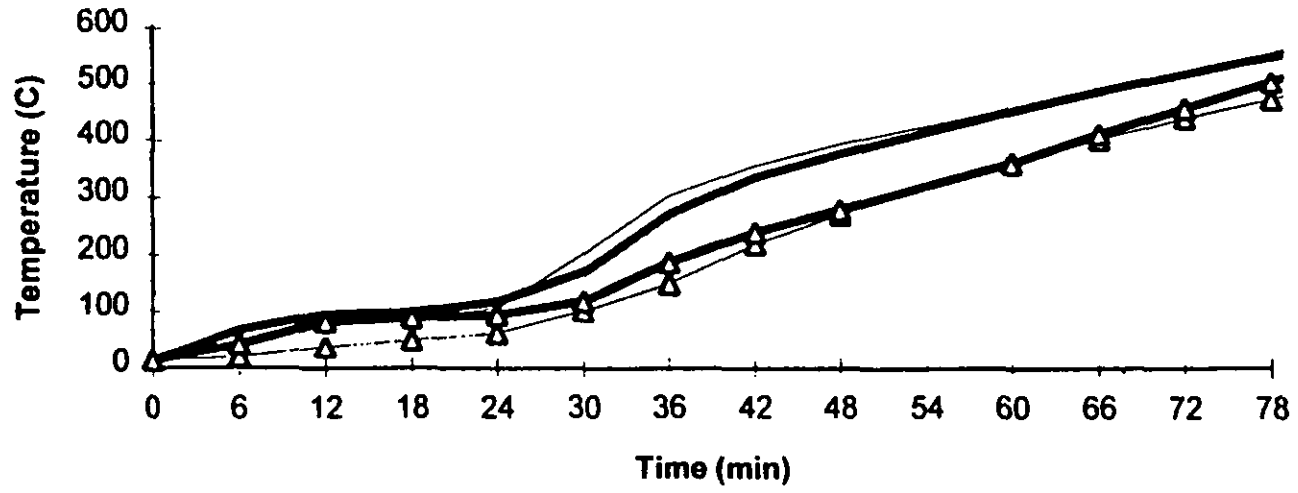

(a) Test 1

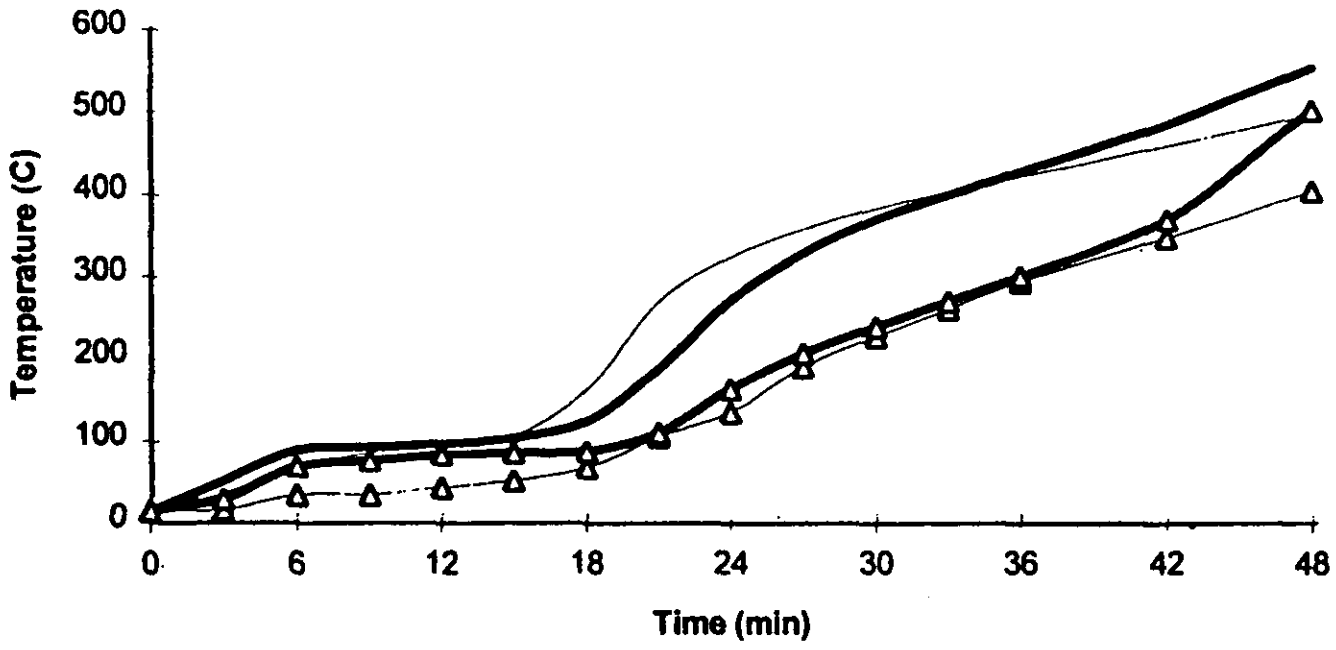

(b) Test 2

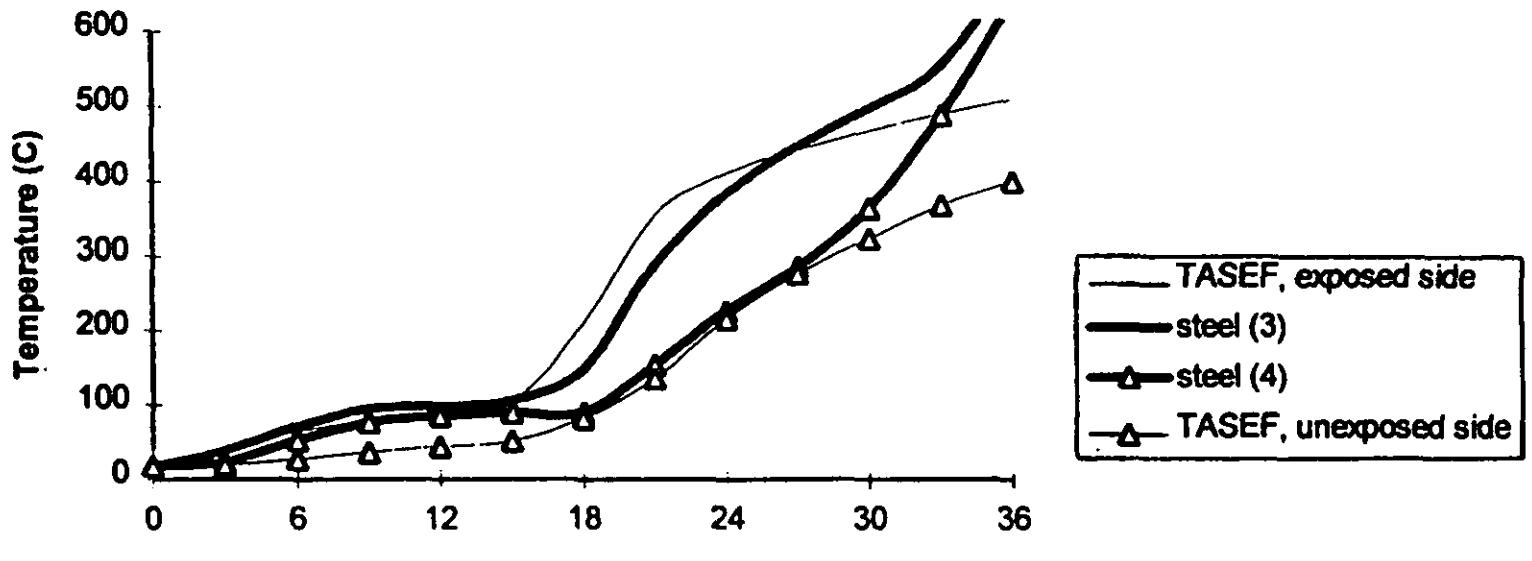

(c) Test 3

Figure 12. Calculated and measured temperatures on flanges of steel studs.

Figure 15 shows the average horizontal deflection along the two central studs. Horizontal deflections were towards the fire. Polynomial curves have been fitted to illustrate the curvature at two different time intervals. Horizontal deflections of the specimen were recorded manually at 10- or 15-minute intervals by means of theodolite readings. For test 1 manual readings were taken at the ends and at 1/4 points along the studs. For tests 2 and 3 manual readings were taken at the ends and at 400 mm centres (1/9 points) along the studs. Linear potentiometers located at mid-height on the unexposed lining provided continuous electronic readings of horizontal mid-span deflection of all four load-bearing studs.

Figure 16 shows the average vertical movement of the bottom platen due to thermal expansion of the studs. A continuous record of the vertical displacement of the loading platen was obtained from linear potentiometers at each end of the platen.

Failure modes

Stability failure as defined by ISO 834[1] was initiated in all cases by structural collapse of the studs. This was followed by an integrity failure of the unexposed lining due to excessive deflections at the locations of stud

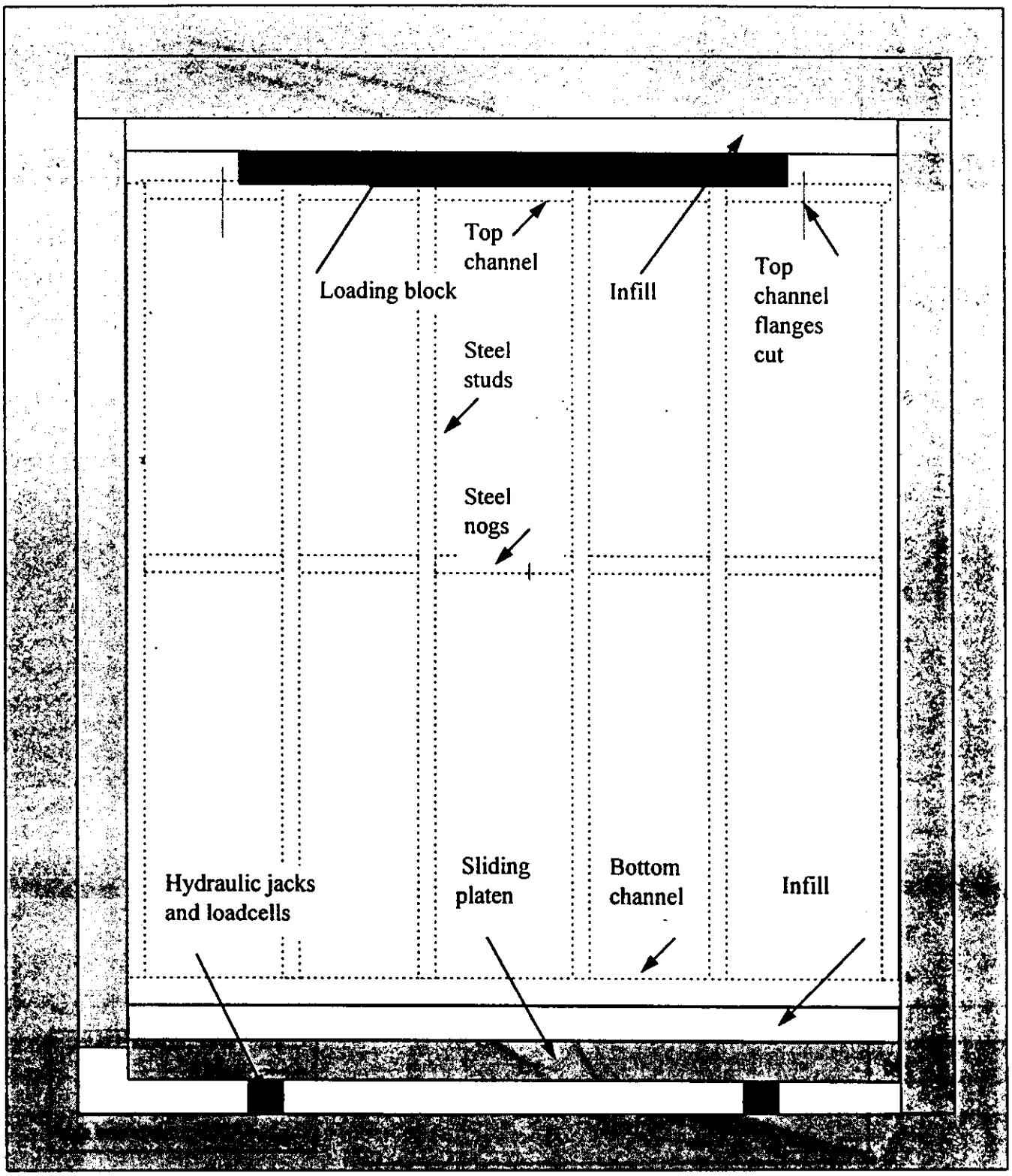

Figure 13. Test arrangement for load-bearing walls.

Table 2. Full scale fire test specimens

Test Number	1	2	3
Lab Number	FR2020	FR2028	FR2031
Wall height (mm)	2850	3600	3600
Steel grade (MPa)	300	450	450
Framing type	C-section	lipped C-section	lipped C-section
Framing (mm)	76 × 32 × 1.15	102 × 51 × 1.0	102 × 51 × 1.0
Load (kN/stud)	6	16	12
Lining thickness exposed (mm)	16.0	12.5	12.5
Lining thickness unexposed (mm)	16.0	12.5	9.5
Fire curve	ISO 834	ISO 834	'severe'

buckling. For all three tests failure was by buckling of the cooler stud flange on the ambient side of the specimen near mid-span. This is the flange with the higher compressive stresses because deflection is towards the fire.

The failure mode for tests 1 and 2 was flexural buckling about the major axis initiated by local buckling of the compression flange between fasteners adjacent to the ambient face lining. The failure mode for test 3 was

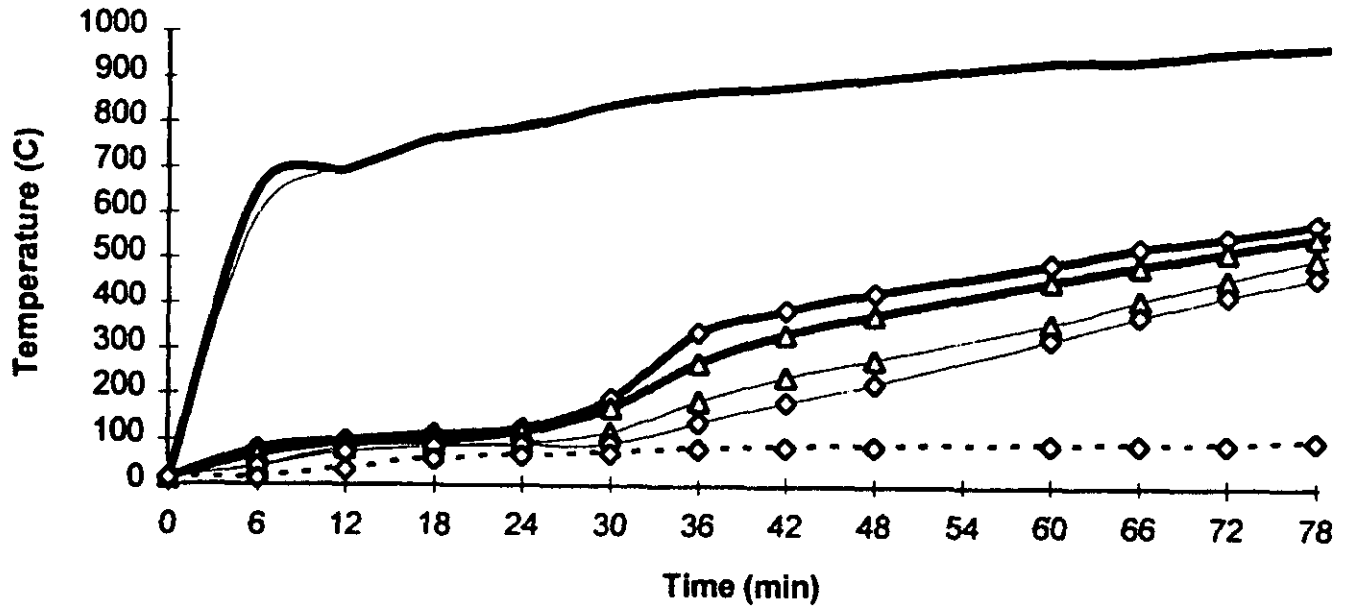

(a) Test 1

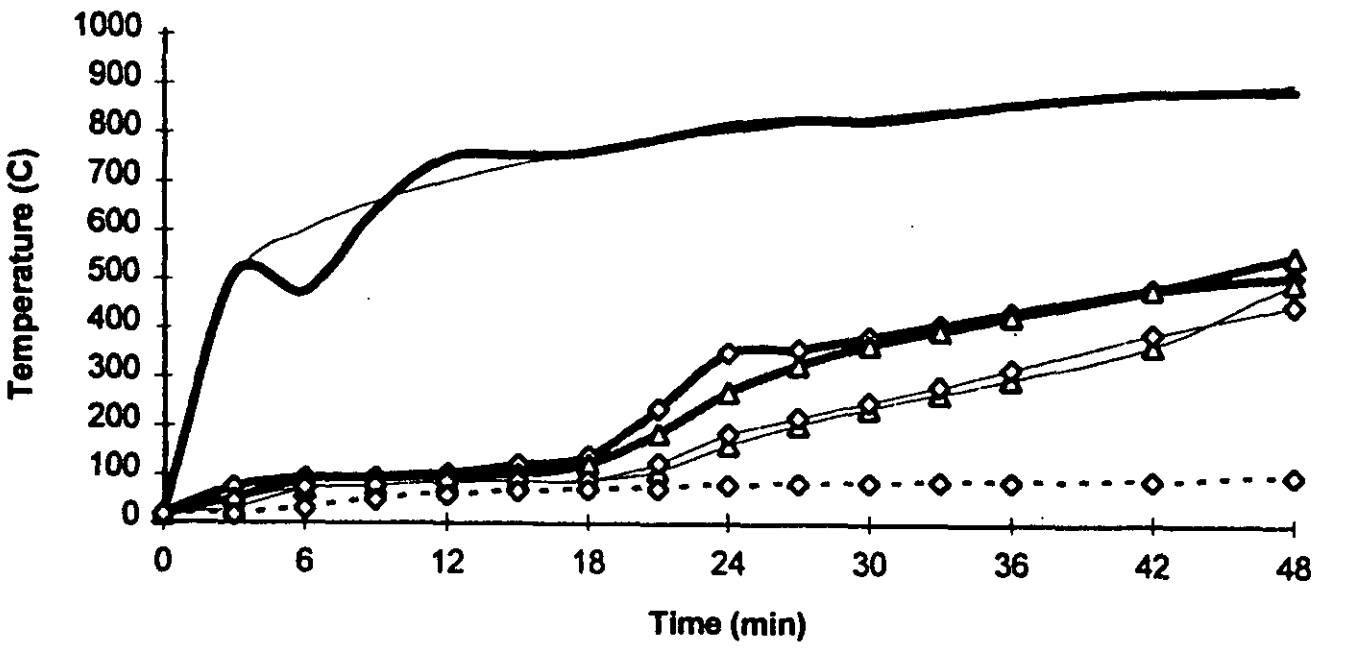

(b) Test 2

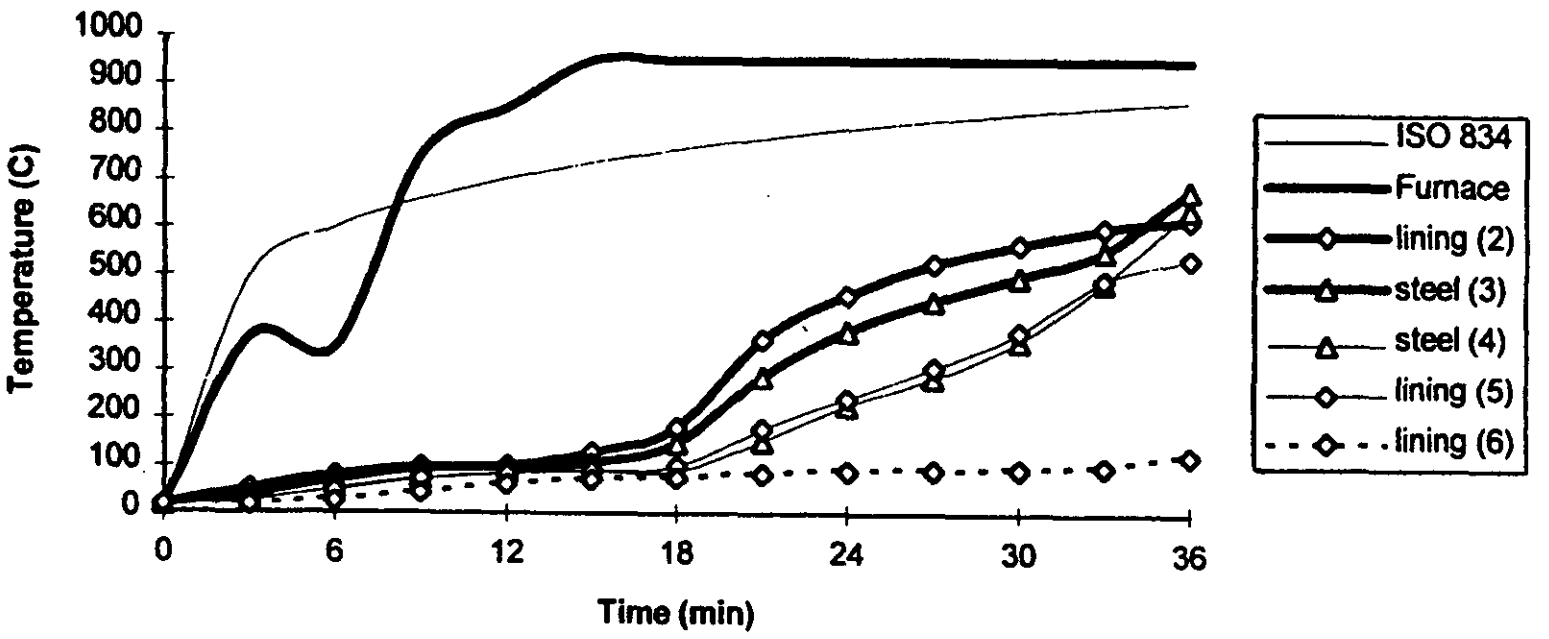

(c) Test 3

Figure 14. Measured temperatures within full-scale test specimens (numbers in brackets indicate temperature measurement position in accordance with Fig. 11).

torsional flexural buckling after the ambient face lining failed to provide lateral restraint to the compression flange.

Structural failure was not clearly defined in test 1. At about 72 minutes a marked increase in horizontal deflections and a reversal in vertical movement was observed, indicating failure of the load-bearing studs. However, load was redistributed through diaphragm action of the ambient face lining to the cooler edge studs which were supported by friction against the specimen holder. In tests 2 and 3 the applied stud load was significantly higher and the effect of friction was minimized and failure

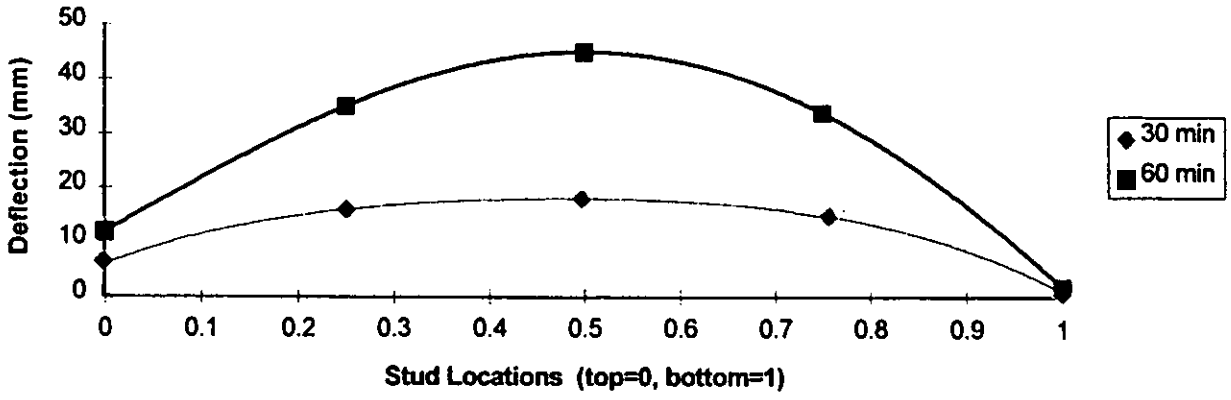

(a) Test 1

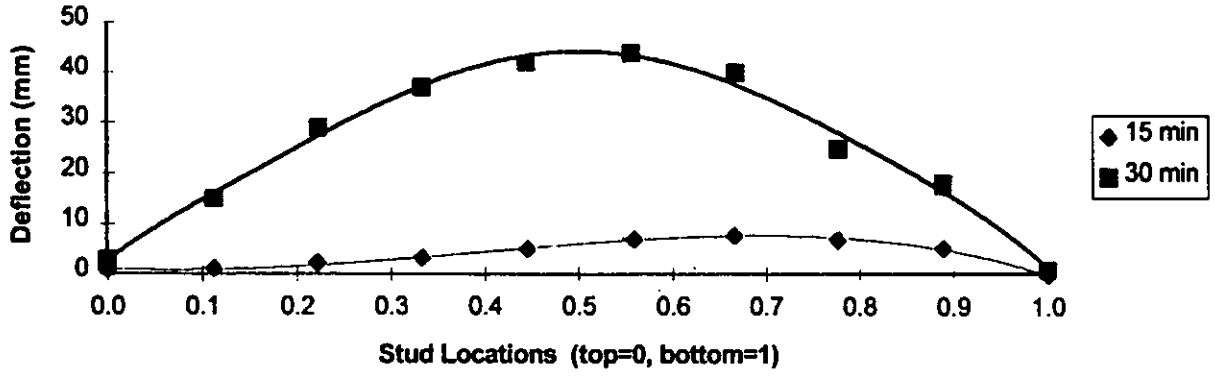

(b) Test 2

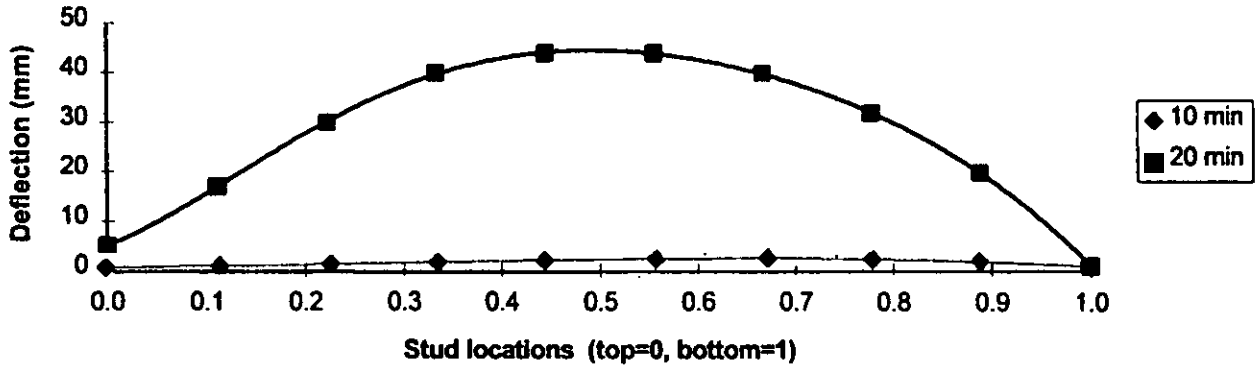

(c) Test 3

Figure 15. Measured horizontal deflection of studs.

was much more sudden. Table 3 gives the failure times for the tests. Structural failure is defined by the reversal in vertical movement.

Discussion of test results

For the two ISO 834[1] tests, measured temperatures throughout the specimen were generally in accordance with TASEF[15] predictions as shown in Fig. 12. These temperatures were consistent with expectations based on previous testing of non-load-bearing LSF walls.[19–21]

After a short initial cooler phase the input fire for test 3 was significantly hotter than the ISO 834 curve. Figure 12(c) shows that measured temperatures were higher than TASEF predictions after 25 minutes. Viewing holes in the test furnace showed that cracking of the exposed lining in test 3 was more severe than that observed for the ISO 834 tests.

The measured mid-span horizontal deflections shown in Fig. 15 give no indication of double curvature near failure and do not provide evidence of significant restraining moments. It is concluded that thermal deflections override rotational restraint provided by

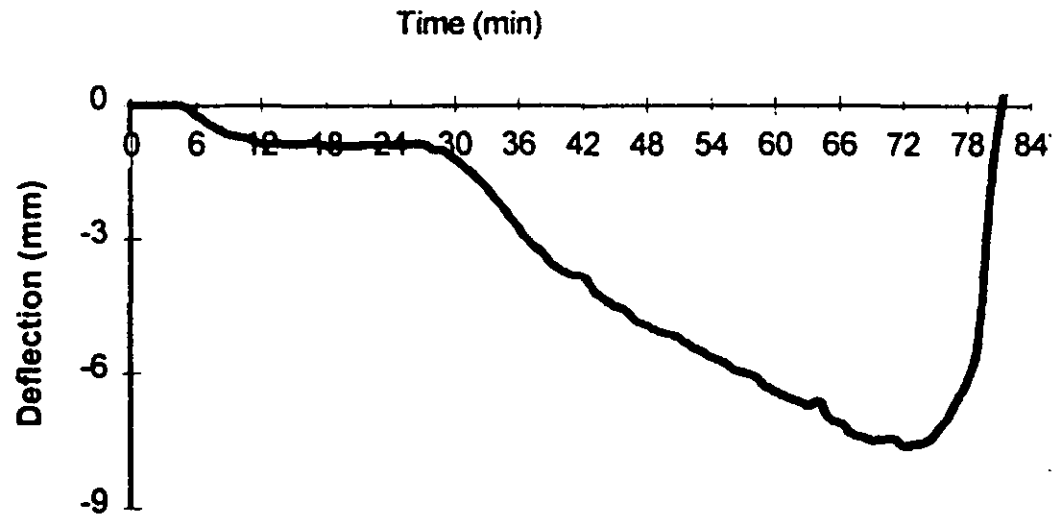

(a) Test 1

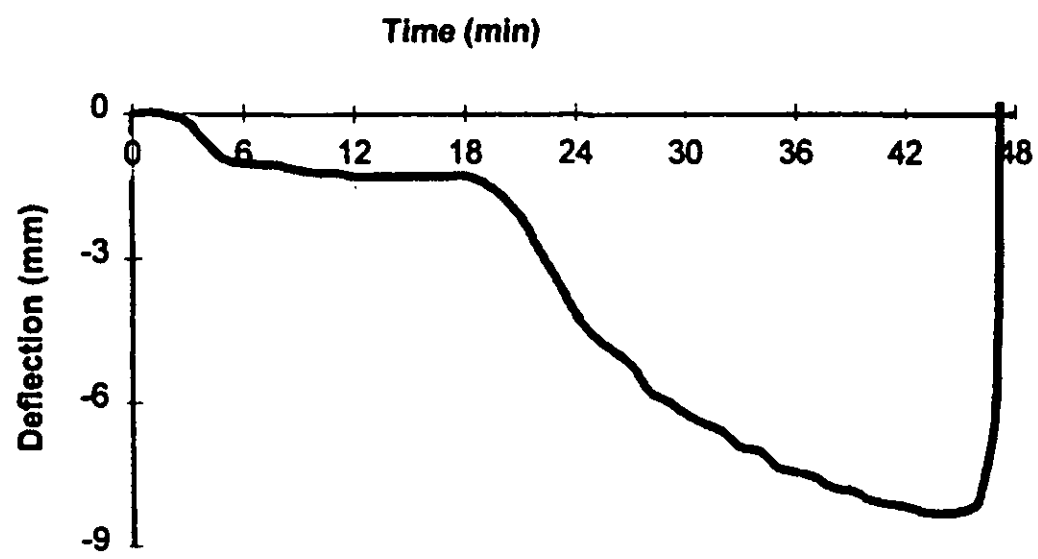

(b) Test 2

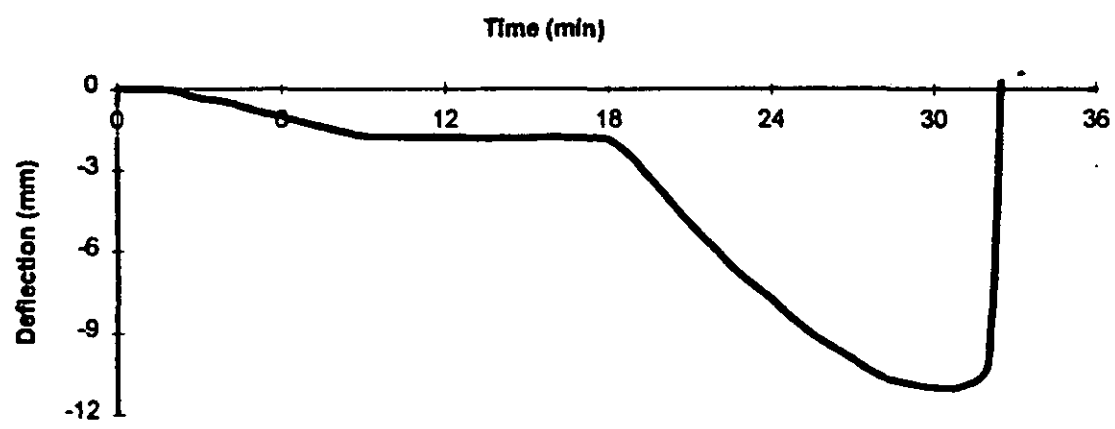

(c) Test 3

Figure 16. Measured vertical movement of bottom platen.

Table 3. Summary of failure times for the full-scale fire tests

Test number	Structural failure (min)	Integrity failure (min)	Insulation failure (min)
Test 1	72	78	Not reached
Test 2	44	45	Not reached
Test 3	32	32	Not reached

stud-to-channel connections and load relocation. The welded connections tested provide the most rigid detail when compared with other typical stud-to-channel connections shown in Fig. 3. This might be different for steel studs cast into concrete footings, but such systems are outside the scope of this study.

Calculated stresses in the studs are given by the following equations,

For the flange on the fire side:

$$F_{yz} = P_a/A - (P_a \times \Delta_z)/Z_x \quad (9)$$

for the flange on the ambient side,

$$F_{yz} = P_a/A + (P_a \times \Delta_z)/Z_x \quad (10)$$

where,

F_{yz} is the calculated steel stress (MPa) at height z

P_a is the applied axial load (N)
A is the cross sectional area of the stud (mm^2)
Δ_z is the measured total horizontal deflection (mm) at height z
Z_x is the section modulus about the X-axis (mm^3)

An example of calculated stresses as a function of time is given in Fig. 17, showing stresses at mid-height and at the stud ends for test 2. Compressive stresses are positive.

Test 3 was designed to achieve an insulation failure with the unexposed lining thinner than the exposed lining. However, after this thin unexposed lining degraded, it failed to provide lateral support to the screws restraining the compression flange of the studs. This resulted in pull-through of the fasteners and torsional flexural buckling of the studs. Examination of the unexposed lining after the test showed a remaining undamaged gypsum layer of about 2 mm.

A method is required to predict the minimum thickness of undamaged lining required to provide lateral restraint against buckling of the steel studs about the minor axis. Design codes provide no detailed information. Indicative minimum load resistance levels in BS 5950[3] require a total lateral restraint of 3% of the compressive load in the critical flange, provided that the load resistance at each point of restraint is not less than 1%. In the absence of detailed information it is proposed that a minimum thickness of the unexposed lining should remain undamaged to prevent lateral buckling. This was modelled by including a finite element grid at this location and limiting the temperature to 100°C. From a comparison of TASEF runs and test results it is proposed that a 3 mm thickness of undamaged gypsum be retained. Note that the provision of glass-fibre reinforcing is essential to prevent pull-through of screws in heat-affected gypsum plasterboard.

THE PROPOSED MODEL

Limiting temperature

The current practice of predicting the performance of load-bearing LSF walls is by limiting the steel temperature to 400°C. This ensures that the steel yield strength is not reduced to less than about 60% of ambient values. This is conservative for most applications when comparing the ratio of fire design load to stud capacity. Limiting steel temperature does not take into account thermal deflections and resulting P-Δ effects. Neither does it consider temperature effects on the modulus of elasticity of steel, which is important in buckling analysis. Limiting temperature is believed to give conservative predictions, but the margin of safety is unknown.

The proposed model

The proposed model consists of two main components:

(1) Heat transfer modelling is used to establish the temperature distribution and time–temperature history of the steel framing.
(2) A spreadsheet is used for the structural analysis of steel studs subjected to a combination of axial loading and bending, while exposed to elevated temperatures.

The predicted horizontal deflections using TASEF[15] temperatures exceed those calculated from measured temperatures. This is because TASEF does not model mass transfer which results in low predicted temperatures on the ambient side of the wall and a greater temperature gradient across the steel stud during the early stages of fire. A linear correlation exists between the temperature gradient and thermal deflection. Greater predicted deflections result in increased steel stresses due to P-Δ effects. Using TASEF temperatures therefore results in conservative failure predictions. An example of deflections calculated from TASEF and measured temperatures is given in Fig. 18. The *thermal deflections* are calculated from the temperature gradient across the steel studs but remain constant after reaching the maximum calculated value. The *total deflections* include P-Δ effects.

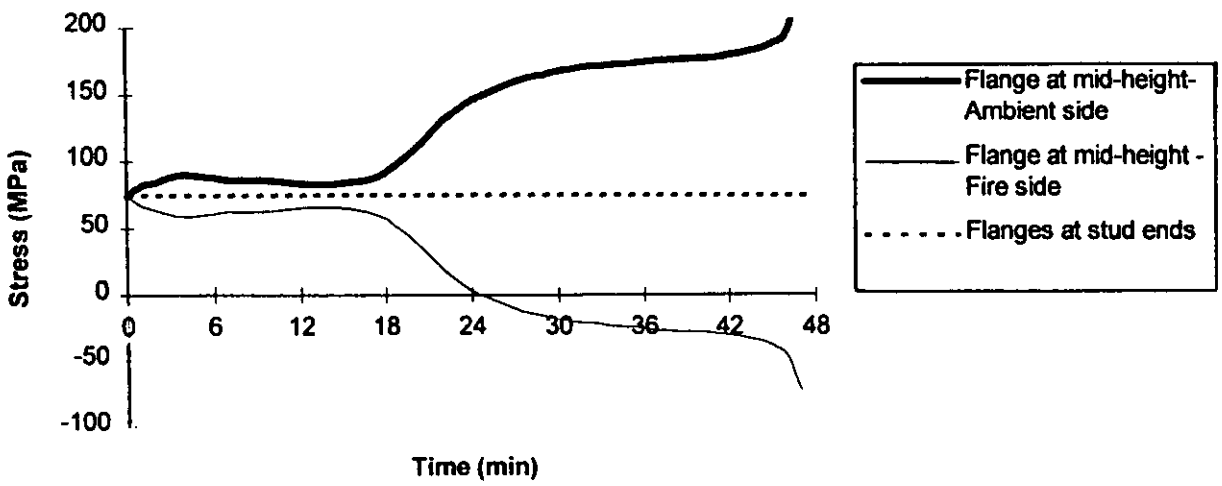

Figure 17. Variation in steel stud stresses with time for test 2.

Comparison with Fig. 9 shows that using TASEF temperatures results in deflection predictions which are higher than those expected in practice.

Structural analysis

A spreadsheet has been developed based on the AISI[5] design manual equations, modified to take into account temperature by adjusting the input values for yield strength and modulus of elasticity as a function of temperature using Eqns (1) and (2) respectively.

The thermal deflection resulting from the temperature gradient across the stud is calculated using Eqn (5). The mean stud temperature is entered to calculate the coefficient of thermal expansion in accordance with Eqn (3). Calculated thermal deflections are conservatively assumed to remain constant when temperature gradients decrease. This is achieved by not allowing the calculated value for a given time step to be less than the previous step. The total horizontal deflection is calculated by adding to the thermal deflection the P-Δ deflection calculated in accordance with Eqn (7). The total deflection multiplied by the applied load gives the maximum stud bending moment. Any lateral loads may be entered as required.

Using the spreadsheet, a critical temperature is found at which the predicted strength of the stud is equal to the applied axial load. This temperature is compared with the compression flange temperature on the ambient side of the wall to find the time to failure.

Real fires

The proposed method can be used for any time–temperature representation of real fires, as well as for the ISO 834[1] fire demonstrated here.

Design example

This example follows the prediction of the failure time for the wall assembly tested in Test 1. Figure 19 shows the steel framing temperature from TASEF and the predicted thermal deflection. The maximum calculated thermal deflection of 26 mm occurs at 36 minutes and is assumed to be constant for the remainder of the test.

From the spreadsheet analysis it is established that for a 26 mm calculated thermal deflection, the critical compression flange temperature is 378°C. When the compression flange reaches this temperature, the axial load

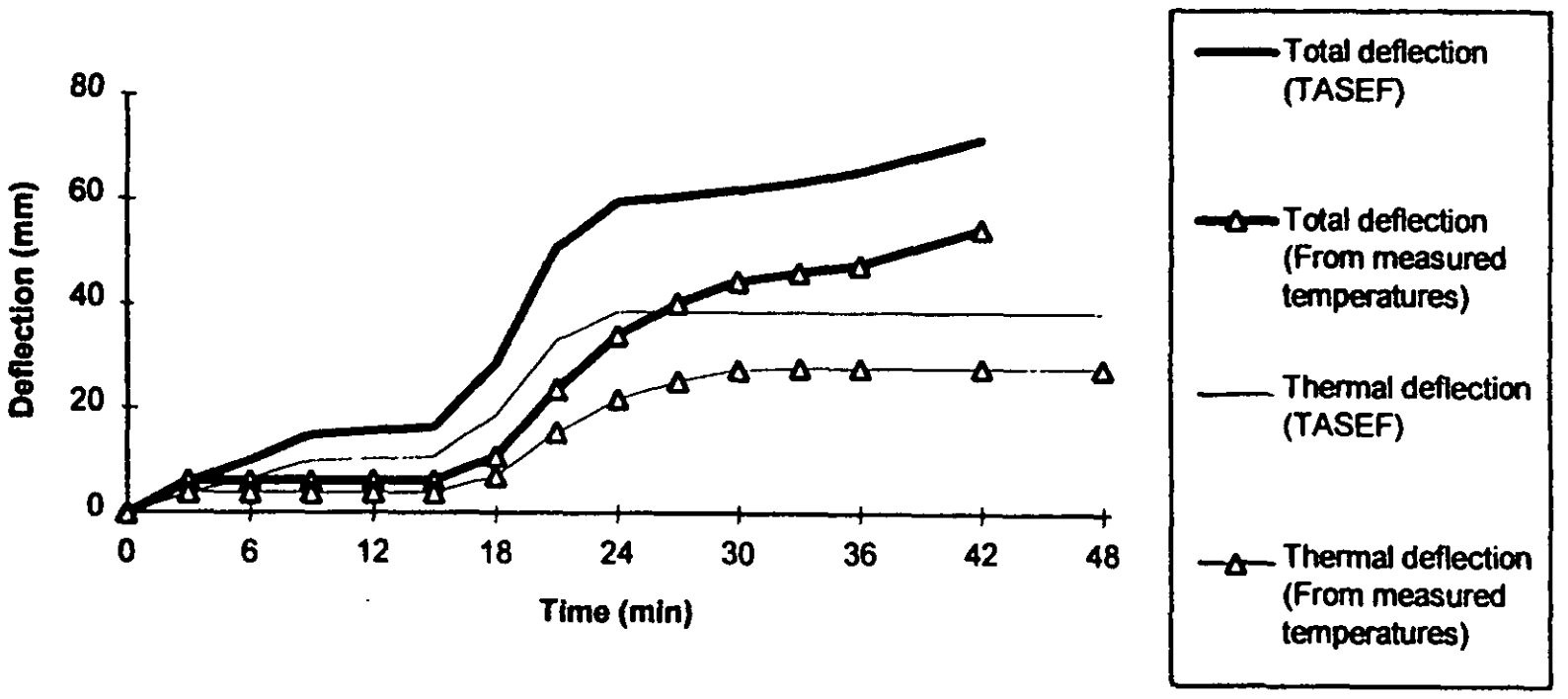

Figure 18. Comparison of calculated horizontal deflections based on TASEF and measured temperatures (test 2).

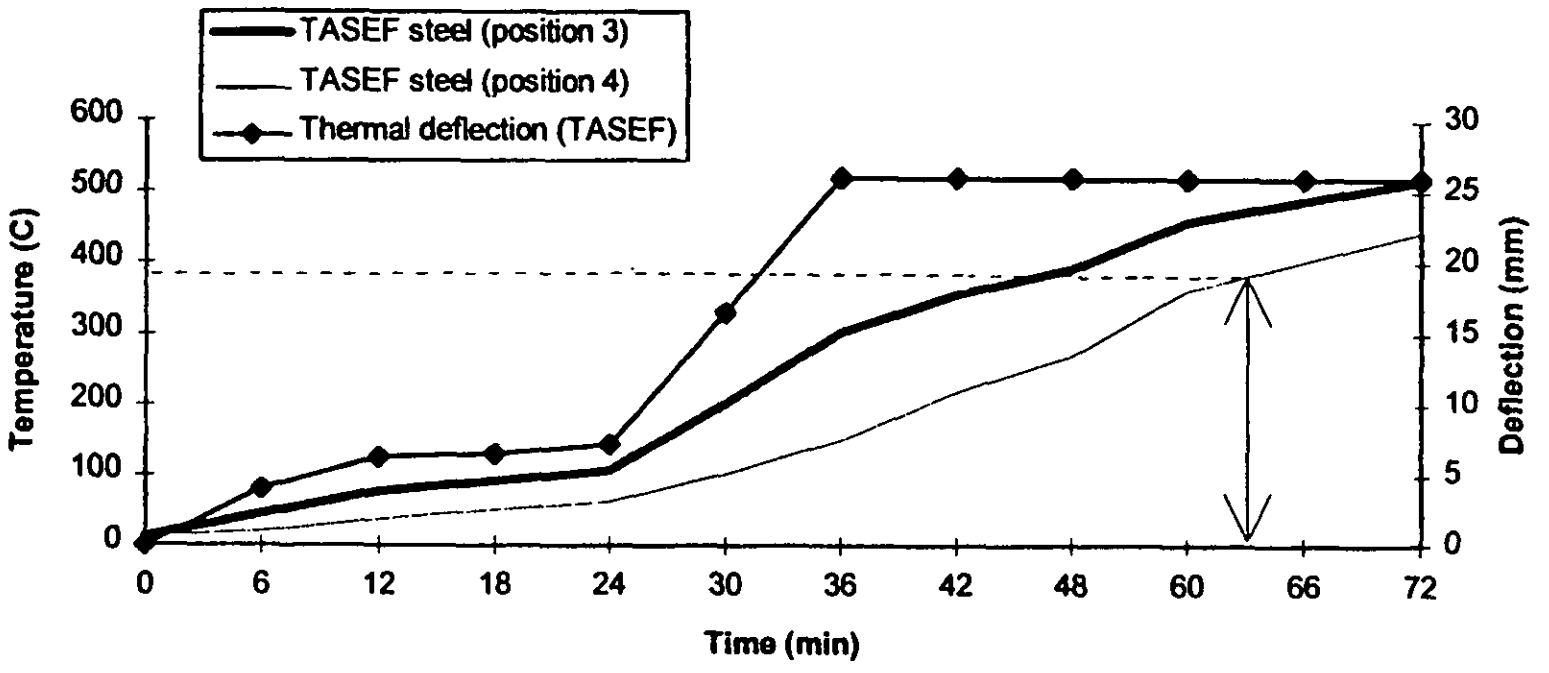

Figure 19. Predicted steel temperatures and thermal deflection (test 1).

capacity of the stud will have dropped to be approximately equal to the applied load. From the bottom curve in Fig. 19 it can be seen that the compression flange will reach 378°C after 63 minutes. This is the predicted time for structural failure by flexural buckling about the major axis, assuming sufficient lateral restraint to prevent lateral buckling.

From TASEF predictions the unexposed lining will provide lateral restraint to the compression flange for 65 minutes. The predicted failure time is therefore governed by flexural buckling about the major axis at 63 minutes. This compares with an observed structural failure at 72 minutes.

Graphical method

The proposed model has been used to predict the failure of load-bearing LSF systems lined with 12.5 mm, 16 mm, and 19 mm glass-fibre reinforced gypsum plasterboard, exposed to the ISO 834 fire. Figure 20 shows the output for various ratios of applied load to design stud capacity. It is suggested that a straight line drawn between a load ratio of unity and an approved rating for a non-load-bearing system[22] be adopted as a quick but conservative estimate of the fire resistance rating of loadbearing steel frame walls. Figure 20 shows that, in accordance with the graphical method, the predicted failure time for test 1 is 45 minutes and for test 2 failure is predicted to occur at 32 minutes. The test results were 72 minutes and 44 minutes respectively.

SUMMARY AND CONCLUSIONS

Summary

The study was carried out to gain understanding of the performance of load-bearing light steel frame (LSF) walls and to model their performance against the ISO 834 and real compartment fires. Structural testing at room temperature was carried out to check relevant structural design codes. The effect of temperature on the steel strength and stiffness was investigated. In order to predict stud bending moments, analytical methods are proposed for calculating the thermal deflection arising from a temperature gradient across the steel members and the superimposed deflection due to P-Δ effects. Heat transfer modelling using TASEF was carried out to predict steel framing temperature. Three full-scale furnace tests were carried out to evaluate the proposed model against the ISO 834 time–temperature curve and a significantly hotter test fire.

General conclusions

Conclusions from the literature

(1) The AISI design manual provides the most recent and reliable source for predicting the ultimate limit state conditions of cold-formed steel studs at room temperature. Structural designs in accordance with the AISI manual were found to be reasonably conservative.
(2) No reliable data exist on the performance of load-bearing LSF walls exposed to fire. The most relevant information was produced by the AISI. However, the AISI information did not allow for freedom of stud expansion and, as a result, fire test loads increased to twice the intended loads.

Conclusions from testing and modelling

(1) Thermal deflections as a result of temperature gradients and deflections due to P-Δ effects can be predicted with good accuracy.
(2) Finite element heat transfer modelling by computer can predict the time–temperature history of LSF systems exposed to fire with reasonable accuracy. Refinement is needed for modelling against fires which are significantly hotter than ISO 834 conditions.
(3) The failure mode of steel studs in LSF systems exposed to fire is generally governed by buckling of the compression flange on the ambient side of the wall assembly.

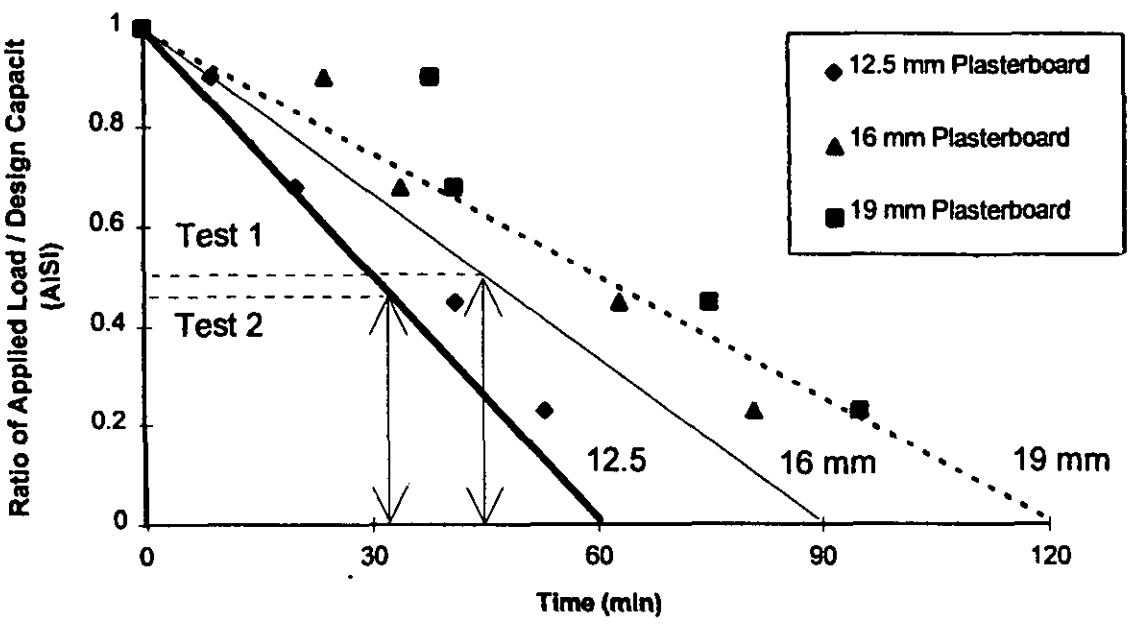

Figure 20. Proposed graphical method.

(4) Thermal deflections override any rotational restraints provided by stud-to-channel fixings.
(5) Walls with low levels of axial load may perform better in fire tests than in actual fire situations because frictional restraints and redistribution of load can enhance the test result.
(6) The current practice of limiting the steel flange temperature on the fire side of the wall assembly is unduly conservative for low load ratios.
(7) A simple graphical design method is proposed for quick reference by designers.
(8) A model is proposed which consists of finite element heat transfer modelling using TASEF to predict steel framing temperatures and a structural analysis using spreadsheets. The model gives conservative predictions of failure times, considered satisfactory for design purposes.

NOTATION

A section gross area (mm^2)
c specific heat ($J\,kg^{-1}°C$)
D section depth (mm)
e enthalpy (MJ/m^3)
E_0 steel modulus of elasticity at ambient temperature (MPa)
E_T steel modulus of elasticity at elevated temperature T(MPa)
F_{y0} steel yield stress at ambient temperature (MPa)
F_{yT} steel yield stress at elevated temperature T(MPa)
F_{yz} steel yield stress at height z(MPa)
I_x moment of area about the x-axis (mm^4)
I_y moment of area about the y-axis (mm^4)
k thermal conductivity ($W\,m^{-1}°C$)
L member length (mm)
P_a applied axial load (kN)
q rate of heat transfer (heat flux)($kW\,m^{-2}$)
T temperature (°C)
T_g gas temperature (K)
T_s surface temperature (K)
W section width (mm)
X_e section shear centre (mm)
X_c section centroid (mm)
Z_x section modulus about the x-axis (mm^3)
Z_y section modulus about the y-axis (mm^3)
α_T coefficient of thermal expansion at temperature T ($°C^{-1}$)
β convection coefficient ($W\,m^{-2}K^{\gamma}$)
δT temperature difference (°C)
Δ_1 deflction due to thermal bowing (mm)
Δ_2 deflection due to P-Δ effects (mm)
Δ_z deflection at height z (mm)
ε emissivity (dimensionless)
γ convection power (dimensionless)
σ Stefan–Boltzmann constant ($5.67*10^{-8}\ W\,m^{-2}\,K^4$)

Acknowledgements

This study was carried out in partial fulfilment of the requirements for the degree of Master of Engineering at the University of Canterbury, Christchurch, and in conjunction with BRANZ (the Building Research Association of New Zealand), Wellington. The testing was performed at the fire research facilities of BRANZ. Financial support was provided by the Foundation for Research, Science and Technology from the Public Good Science Fund, from the Building Research Levy, and from Winstone Wallboards Ltd, Auckland. Materials for testing were donated by Steel Technology Ltd and Winstone Wallboards Ltd.

REFERENCES

1. ISO *Fire Resistance Tests—Elements of Building Construction*. International Standard ISO 834 (1975).
2. J. T. Gerlich Design of loadbearing light steel frame walls for fire resistance. Fire Engineering Research Report 95/3, University of Canterbury. Christchurch, New Zealand (1995).
3. AS 1538: Cold-Formed Steel Structures Code. Standards Association of Australia. North Sydney, NSW, Australia (1988).
4. BS 5950: Part 5 : Structural Use of Steelwork in Building. Part 5. Code of practice for Design of Cold-Formed Sections. British Standards Institution. London (1987).
5. Load and Resistance Factor Design Specification for Cold-Formed Steel Structural Members. American Iron and Steel Institute. Washington, DC (1991).
6. G. C. Thomas, A. H. Buchanan, A. J. Carr, C. M. Fleischmann, and P. J. Moss, Light timber framed walls exposed to compartment fires. *Proceedings, Pacific Timber Engineering Conference*. Volume 2, pp. 531–538. Timber Research and Development Advisory Council. Queensland, Australia (1994).
7. J. R. Mehaffy, *Development of Fire Endurance Models for Wood Stud Walls—Progress Report*, Forintek Canada Corporation.
8. J. Milke, *Analytical Methods for Determining Fire Resistance of Steel Members*, The SFPE Handbook of Fire Protection Engineering, pp. 3/88–3/112. Society of Fire Protection Engineers. Quincy, MA (1988).
9. K. H. Klippstein, *Strength of Cold-Formed Studs Exposed to Fire*, American Iron and Steel Institute. Washington, DC (1980).
10. T. T. Lie, *Structural Fire Protection*, American Society of Civil Engineers. New York (1992).
11. Y. Anderberg, *Properties of Materials at High Temperatures, Steel*, Division of Building Fire Safety and Technology. Lund Institute of Technology. Lund, Sweden (1983).
12. G. M. E. Cooke, *Thermal Bowing and how it Affects the Design of Fire Separating Construction*, Fire Research Station. Building Research Establishment. Herts (1987).
13. P. C. R. Collier, *A Model for Predicting the Fire Resistance Performance of Cavity Walls in Realistic Fires*, to be published (1994).
14. P. Clancy, S. Young, V. Beck, and R. H. Leicester, Modelling of timber-framed barriers in real fires. *Proceedings, Pacific Timber Engineering Conference*, Volume 2, pp. 273–282, Timber Research and Development Advisory Council. Queensland, Australia (1994).
15. E. Sterner, and U. Wickstrom, *TASEF—Temperature Analysis of Structures Exposed to Fire*, Fire Technology SP Report 1990:05, Swedish National Testing Institute. Boras, Sweden (1990).
16. AS 1530: Part 4 : Fire Resistance Tests of Elements of Building Construction. Standards Association of Australia. North Sydney, NSW, Australia (1990).
17. K. H. Klippstein, *Behaviour of Cold-Formed Steel Studs in Fire Tests*, American Iron and Steel Institute. Washington, DC (1980).

18. ASTM E119-79: Standard Methods of Fire Tests of Building Construction and Materials. American Society for Testing and Materials. Philadelphia (1979).
19. Branz, FR 1411: Report on the fire resistance properties of a non-loadbearing steel framed wall lined with one layer of 19 mm Fyreline Gibraltar Board. Judgeford, New Zealand, confidential report for Winstone Wallboards Ltd (1988).
20. Branz, FR 1579: Report on the fire resistance properties of a non-loadbearing steel framed wall lined with 12.5 mm Fyreline Gibraltar Board. Judgeford, New Zealand, confidential report for Winstone Wallboards Ltd (1990).
21. Branz, FR 1722: Report on the fire resistance properties of a non-loadbearing steel framed wall lined with two layers of 12.5 mm Fyreline Gibraltar Board. Judgeford, New Zealand, confidential report for Winstone Wallboards Ltd (1992).
22. Winstone Wallboards Ltd, *Gib® Board Fire Rated Systems, 1992*, Auckland, New Zealand (1992).

Design of light steel-framed walls for
fire resistance.
GERLICH, J.T.
1996 34643

BRANZ

THE RESOURCE CENTRE FOR BUILDING EXCELLENCE

BRANZ MISSION

To be the leading resource for the development of the building and construction industry.

HEAD OFFICE AND RESEARCH CENTRE

Moonshine Road, Judgeford
Postal Address - Private Bag 50908, Porirua
Telephone - (04) 235-7600, FAX - (04) 235-6070

REGIONAL ADVISORY OFFICES

AUCKLAND
Telephone - (09) 526 4880
FAX - (09) 526 4881
419 Church Street. Penrose
PO Box 112-069, Penrose

WELLINGTON
Telephone - (04) 235-7600
FAX - (04) 235- 6070
Moonshine Road, Judgeford

CHRISTCHURCH
Telephone - (03) 366-3435
FAX (03) 366-8552
GRE Building
79-83 Hereford Street
PO Box 496